Journal of Hazardous Materials 223–224 (2012) 79–83

Contents lists available at SciVerse ScienceDirect

Journal of Hazardous Materials

journal homepage: www.elsevier.com/locate/jhazmat

Enhanced photoelectrocatalytic activity for dye degradation by graphene–titania composite film electrodes

Peifang Wang, Yanhui Ao*, Chao Wang, Jun Hou, Jin Qian

Key Laboratory of Integrated Regulation and Resource Development on Shallow Lakes, Ministry of Education, College of Environment, Hohai University, Nanjing 210098, China

ARTICLE INFO

Article history:
Received 13 October 2011
Received in revised form 20 April 2012
Accepted 23 April 2012
Available online 27 April 2012

Keywords:
Graphene
Photo-electrocatalysis
Titania
Composite film electrode

ABSTRACT

Graphene–titania composite film electrodes have been fabricated by a dip-coating method. Transmission electron microscopy (TEM) images show that the titania nanoparticles were dispersed uniformly, with only a little aggregation on the surface and edges of the graphene sheets. XRD analysis showed that the composite electrodes comprised the anatase phase of titania with just a little rutile phase. The photoelectrocatalytic activities of the as-prepared samples were investigated by studies of the degradation of Reactive Brilliant Red dye X-3B (C.I. reactive red 2). An enhancement of the photocurrents was observed using the graphene–titania composite electrodes, compared with pure titania film electrodes, under UV light irradiation. This improvement is attributed to the following two reasons: enhanced migration efficiency of the photo-induced electrons and enhanced adsorption activity of the dye molecules. In addition, we investigated the effects of graphene content and pH values on the photoelectrocatalytic activity of the as-prepared composite film electrodes. Results showed that there was an optimal amount of 5% (initial graphite oxide content).

1. Introduction

Semiconductor photocatalysis has been extensively investigated in environmental issues such as water and air purification [1–6]. Among different semiconductors materials, titania has been proved to be the most promising semiconductor materials due to its chemical stability, low cost and environmental friendliness [7]. However, the quantum yields of the titania based reaction are very low, which prompts the investigations of ways for improving the photocatalytic activity.

In recent years, graphene has received much attention because of its remarkable properties [8–12]. It has been reported that the theoretical value of the specific surface area of graphene is as high as 2630 m^2/g [13]. Therefore, it can serve as an ideal support material with improved interfacial contact and enhanced adsorption activity. It is also well known that graphene has a robust but flexible structure, with high carrier mobility. Thus, a titania–graphene composite material should show excellent photocatalytic activity. Graphene can be easily obtained from graphite, which is cheap and widely available. Some previous investigations of the preparation and properties of titania–graphene composite materials have been published [14–17].

The photoelectrocatalytic process takes advantage of the photocatalytic process by applying a biased voltage across a photo-electrode on which the photocatalysts are supported. This technology has been proved to be an efficient method for the degradation of organic contaminants [18–20]. In the photoelectrocatalytic process, photo-induced electrons and holes can be well separated under the influence of the applied electric field if the applied potential is higher than the flat band potential [21]. In most photoelectrocatalytic systems, a pure or doped titania film electrode is used as the photoanode, produced by coating nano-sized titania particles or titania based composites on to a conducting support medium such as indium-tin oxide (ITO) glass, F-doped tin oxide (FTO) or metallic materials [22–26]. Due to the advantages of graphene, the preparation of graphene–titania composite film electrodes might induce further improvement of the activity of titania for the degradation of organics. However, to the best of our knowledge, there have been few reports that have focused on the photoelectrocatalytic degradation of organic pollutants by titania–graphene composite film electrodes.

In the present work, we prepared titania–graphene composite film electrodes using a simple method, in which no calcination is needed to obtain a stable film electrode. Subsequently, we studied their photoelectrocatalytic activity for the decomposition of azo dye X-3B in aqueous solution. Furthermore, we investigated the influence of graphene content on the photoelectrocatalytic activity of the obtained composite film electrodes. The effect of the pH value of the dye solution on the photocatalytic degradation percent of X-3B was also studied.

* Corresponding author. Tel.: +86 25 83787330; fax: +86 25 83787330.
E-mail addresses: andyao@seu.edu.cn, andyao@hhu.edu.cn (Y. Ao).

0304-3894/$ – see front matter © 2012 Elsevier B.V. All rights reserved.
http://dx.doi.org/10.1016/j.jhazmat.2012.04.050

2. Experimental

2.1. Preparation of graphene–titania composite film electrodes

The graphite oxide (GO) was prepared by a modified Hummers method, as reported previously [27]. In a typical synthesis, 2 g graphite powder was put into 100 mL of concentrated H_2SO_4. Then, 8 g $KMnO_4$ was added slowly to the above solution with stirring. The temperature of the mixture was controlled by an ice-water bath and the reaction allowed to proceed for another 2 h. Afterwards, the solution was stirred at 35 °C for 1 h before it was diluted with 100 mL ultrapure water, also in an ice bath. The reaction was allowed to continue for 1 h then the mixture was further diluted to about 300 mL with ultrapure water. Afterwards, 20 mL of 30% H_2O_2 was added slowly to the mixture. Finally, the mixture was filtered and washed with 5% HCl aqueous solution and ultrapure water 5 times. The resulting sample was dried at 60 °C under vacuum.

For the preparation of graphene–titania composite, a definite amount of as-prepared GO was added to a mixture of 50 mL ultrapure water + 25 mL ethanol (in a glass beaker) to form a suspension. This was irradiated for 1 h using an ultrasonic bath-type system (Kunshan, China, 100 W, and 80 kHz). Afterwards, 0.2 g of P25 titania was added to the above suspension and stirred for 2 h. The obtained suspension was transferred and sealed in a 100 mL Teflon-lined autoclave and maintained at 120 °C for 3 h. The graphene–titania composite was then obtained after washing 3 times with ultrapure water. Finally, the graphene–titania composite film electrodes were prepared by a dip-coating method using the composite. First of all, the F-doped tin oxide (FTO, 4 cm × 2 cm) glass was cleaned with acetone, followed by dehydrated alcohol and ultrapure water. The clean FTO glass was immersed in the sol for 15 min, drawn out at a speed of 2 cm min^{-1} and then dried at 333 K under vacuum for 1 h. The process was repeated 5 times. In the present work, three samples, with initial graphite oxide content of 2.5%, 5%, and 10% were prepared; these are denoted as G-P25-1, G-P25-2 and G-P25-3, respectively. For comparison, pure P25 titania was also treated by the same process without the addition of GO.

2.2. Characterization

The structures were determined by X-ray diffraction (XD-3A, Shimadazu Corporation, Japan) using graphite monochromatic copper radiation (Cu–Kα) at 40 kV, 30 mA over the 2θ range 10–80°. The morphologies were characterized by transmission electron microscopy (TEM, JEM2000EX). The concentrations of X-3B in the irradiation process were analyzed using the UV–vis spectrophotometer (Shimadzu 3600).

2.3. Photoelectrochemical measurements

Photoelectrochemical measurements were performed on a CHI 660D electrochemical workstation (Shanghai, Chenhua, China) using a standard three-electrode cell with a working electrode, a platinum wire as counter electrode, and a standard Ag/AgCl in saturated KCl as reference electrode. The working electrodes were the composite film electrodes obtained as described above. The transient photocurrent responses of different samples were recorded using a switch-on and switch-off model. A 250 W high-pressure mercury lamp (Instrumental Corporation of Beijing Normal University) was used as the source of the UV light irradiation. The electrochemical impedance spectroscopies (EIS) were carried out under open circuit potential. The amplitude of the sinusoidal wave was 10 mV, and its frequency ranged from 100 kHz to 0.05 Hz. During all measurements, 0.1 M Na_2SO_4 was used as the electrolyte.

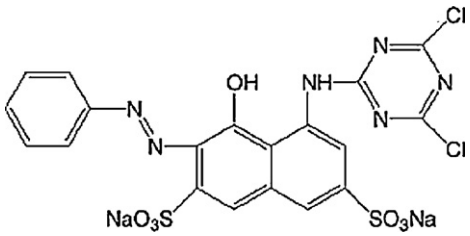

Scheme 1. Molecular structure of dye X-3B (chemical formula = $C_{19}H_{10}O_7N_6C_{12}S_2Na_2$).

2.4. Photoelectrocatalytic (PEC) degradation experiment

The PEC experiments were performed in a rectangular shaped quartz reactor (30 mm × 30 mm × 50 mm) using a three electrode system with saturated Ag/AgCl as the reference electrode, a platinum wire as counter electrode and the graphene–titania composite film as the working electrode. The supply bias and current were controlled using a CHI electrochemical analyzer (CHI660D, Shanghai, Chenghua). A 250 W high-pressure mercury lamp was chosen as the light source and the illumination area was 20 mm × 20 mm. Reactive Brilliant Red X-3B (C.I. reactive red 2) was chosen as model contaminant. The X-3B dye was obtained from Shanghai Dyestuff Chemical Plant and used without further purification. Scheme 1 displays the structure of reactive brilliant red dye X-3B. The initial concentration of X-3B was 10 mg L^{-1} and the reaction solution was 40 mL during the experiment. Before the irradiation, the system was maintained in the dark for 0.5 h to reach complete adsorption–desorption equilibrium (under stirring).

3. Results and discussion

3.1. Characterization of the graphene–titania composite electrodes

Fig. 1 displays typical TEM images of as-prepared graphene–titania composite and pure P25 titania photocatalysts. It clearly shows the 2D graphene sheets and titania nanoparticles (Fig. 1(a)). From the image with higher resolution, we can see that the titania nanoparticles, despite some aggregation, are distributed uniformly on the surface and edges of the graphene sheets (Fig. 1(b)). This is because the titania nanoparticles can interact with the graphene sheets through physisorption, electrostatic binding or through charge transfer interactions [28]. The TEM image of P25 treated by the same process, but without the addition of GO, is also shown in Fig. 1(c). It can be seen that all the titania particles (pure P25 or graphene–titania composite) show similar shapes and diameters.

Fig. 2 shows the XRD patterns of the three G-P25 and pure P25 samples. It can be seen that all samples exhibit the characteristic peaks of the anatase phase of titania (major peaks: 25.4°, 38.0°, 48.0°, 54.7°). In addition, a small amount of the rutile phase can be observed. These XRD patterns are all similar to that of pure P25 (also shown in the figure), which illustrates that the addition of graphene to the P25 titania did not influence the phase structures.

The optical properties of as-obtained samples were investigated by UV–vis diffuse reflectance spectroscopy (DRS). Fig. 3 shows the obtained spectra of the P25 and G-P25 samples. All samples display the typical absorptions with an intense transition in the UV region, which is mediated by the intrinsic band gap absorption of titania resulting from the electron transitions from the valence band to conduction band. From the plot we can also see that the G-P25 samples show similar absorption to that of P25, but there are some red-shifts in the absorption edges of the G-P25 samples compared to pure P25. The red-shift in the absorption edge may

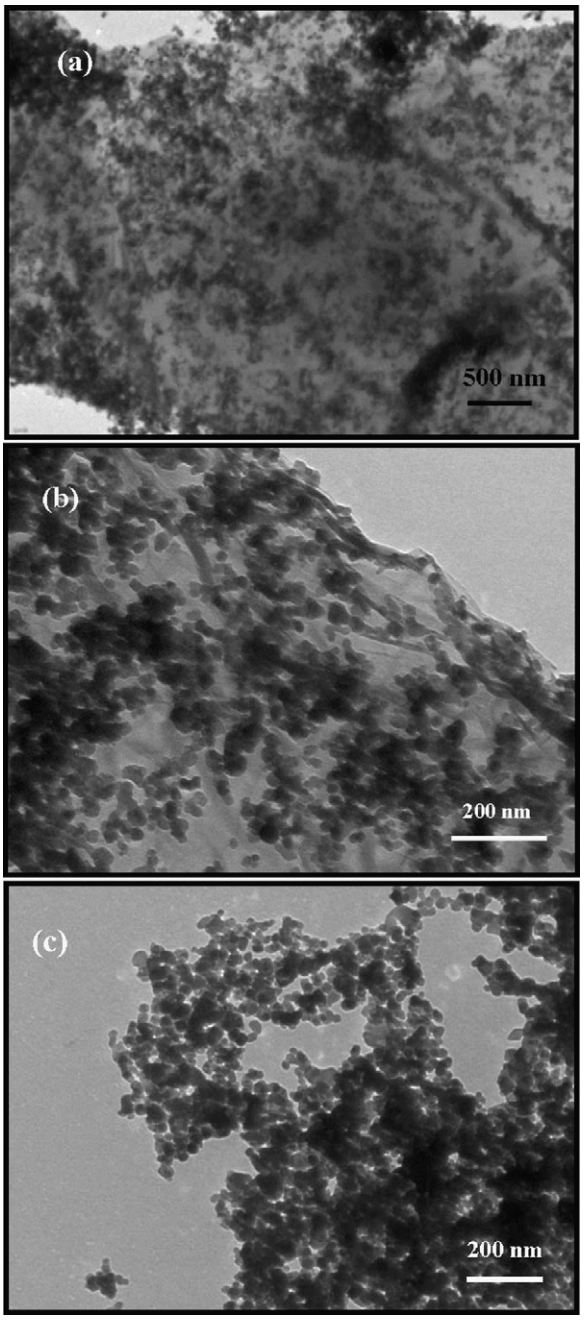

Fig. 1. Typical TEM images of G-P25 and P25 samples.

be induced by the chemical bonding between the titania nanoparticles and graphene. Furthermore, a broad background absorption in the visible light region is observed for the G-P25 samples compared to P25. This can be attributed to the presence of graphene in the composites, since it is a type of carbon. The results are in good agreement with other reports [29,30].

3.2. Photoelectrochemical properties

Photoelectrochemical experiments were performed to investigate the electron interaction between the titania and graphene. Photocurrent measurements were carried out at open circuit potentials using the G-P25 and P25 electrodes, and the results are shown in Fig. 4. A fast and uniform photocurrent response can be observed in all electrodes. Fig. 4 also shows that all G-P25 composite electrodes exhibit a much higher photocurrent density than the

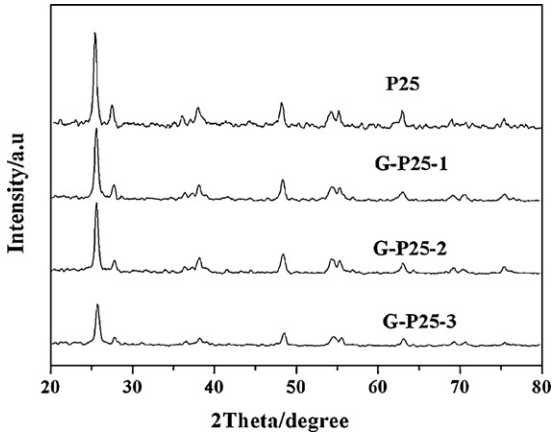

Fig. 2. XRD patterns of G-P25-1, G-P25-2 G-P25-3, and P25.

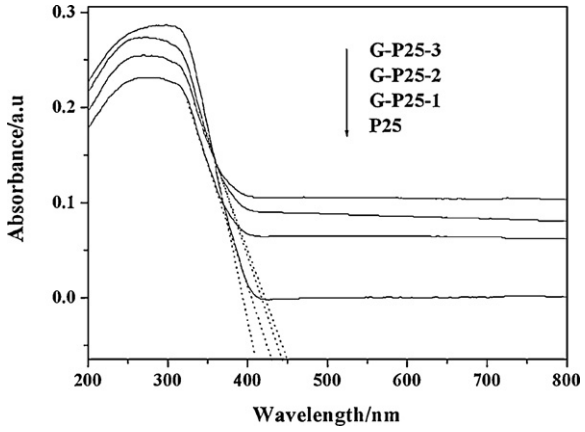

Fig. 3. UV–vis diffuse reflectance spectra of P25, G-P25-1, G-P25-2, and G-P25-3.

pure P25 film electrode. The enhanced photoresponse benefits from the introduction of graphene into the film electrodes. Graphene can accept the photo-induced electrons from P25 and transfer them rapidly to the external circuit, since the graphene has an extensive two-dimensional π–π conjugated structure. Furthermore, we can observe that the photocurrent density is enhanced as the graphene content increases.

A further investigation of the effect of graphene on the photogenerated separation efficiency was carried out by measuring the EIS under UV light at the corresponding open-circuit potential. As shown in Fig. 5, the typical EIS are presented as Nyquist plots. We

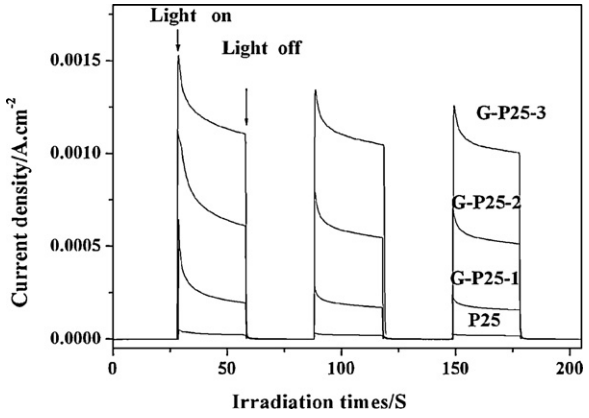

Fig. 4. Photocurrent transient responses of P25, G-P25-1, G-P25-2, and G-P25-3 electrodes.

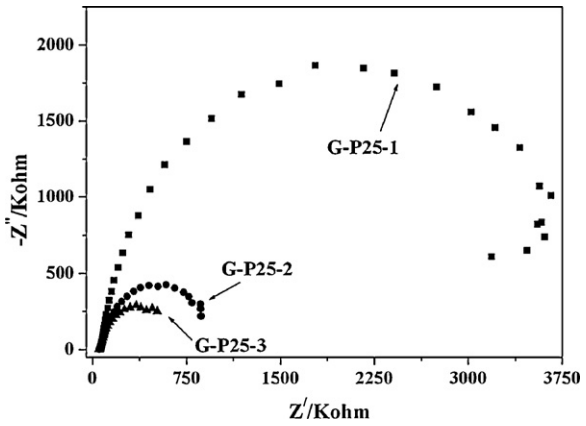

Fig. 5. Electrochemical impedance spectroscopy (EIS) Nynquist plots of G-P25-1, G-P25-2, and G-P25-3 electrodes under UV light irradiation.

can observe that the size of the semicircle in the plot is reduced with increasing graphene content. This indicates that the resistance of the composite film is reduced with increasing graphene content. This means that the interfacial charges can transfer more rapidly and induce effective separation of photo-induced electron–hole charge pairs. The results are in good agreement with the photocurrent measurements.

3.3. Photoelectrocatalytic (PEC) degradation of dye X-3B

We evaluated the photoelectrocatalytic activity of the graphene–titania composite film electrodes in terms of their X-3B degradation efficiency. Before the photoelectrocatalytic experiment, the adsorption and photo degradation of X-3B were investigated. The percentage adsorption of X-3B on G-P25-1, G-P25-2 and G-P25-3 are 7.42%, 9.26% and 10.89%, respectively. In addition, a negligible fraction, less than 2%, photolytic degradation of X-3B was observed after 1 h irradiation. Fig. 6 presents a plot of the dependence of the PEC degradation of X-3B on the applied potentials. The percentage degradation of X-3B by sample G-P25-1 measured at 25 min increases from 36.4% to 71.8% as the applied potential was increased from 0 to 2.0 V (as saturated Ag/AgCl), while the data for G-P25-2 and G-P25-3 are 41.6–78.7%, and 38.3–73.8%, respectively. When no photocatalyst film was applied (i.e. electrolysis), the degradation percentages are 1.3%, 1.5%, 3.6%, 5.6% and 9.7% for bias voltages of 0.3, 0.6, 0.9, 1.2 and 2.0 V, respectively. Therefore, this indicates that most of the X-3B

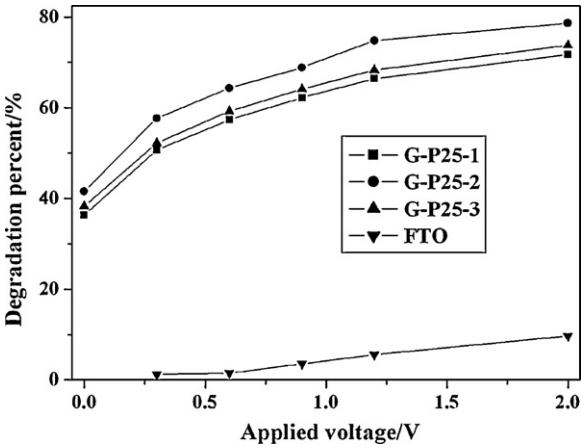

Fig. 6. The effect of applied potentials on the photoelectrocatalytic degradation of X-3B after 25 min irradiation for G-P25 composite electrodes.

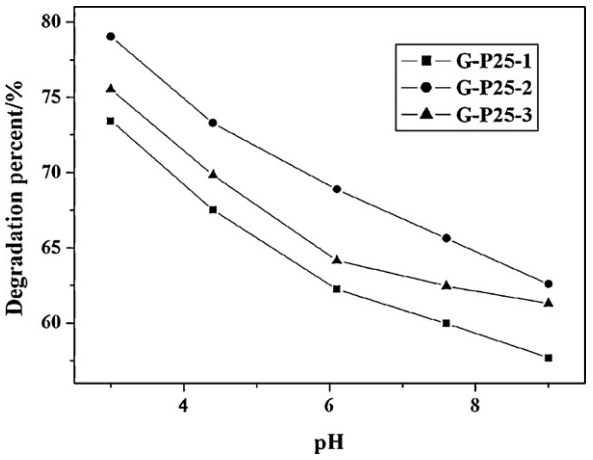

Fig. 7. The effect of pH values on the photoelectrocatalytic degradation of X-3B after 25 min irradiation.

was photoelectrocatalytically degraded for all values of the bias voltage. Applying a bias positive to the flat band potential of a film electrode can result in band bending across the depletion layer, minimizing the probability of recombination of electrons and holes and elevating the PEC efficiency [31]. In the process of photoelectrocatalytic degradation of dyes, the graphene can attract the photo-induced electrons, thus helping to reduce the recombination rate of the photo-generated electron–hole pairs. Furthermore, the electrons can also react with O_2 molecules to produce $^{\bullet}O_2^-$, which can react with H_2O to produce $^{\bullet}OH$. Both $^{\bullet}O_2^-$ and $^{\bullet}OH$ can induce the degradation of dye molecules. Furthermore, we can observe that the degradation efficiency follows the trend: G-P25-2 > G-P25-3 > G-P25-1. This clearly illustrates that it is not more graphene content that induces higher photoelectrocatalytic efficiency; there is an optimal value of graphene content that achieves the highest photoelectrocatalytic activity. This phenomenon can be explained as follows. Graphene is a dark material which can absorb UV light. So superfluous graphene will reduce the absorption efficiency of light by titania nanoparticles. This can be seen from the UV–vis results, showing that G-P25-3 absorbs most light over all visible wavelengths.

In order to determine if this composite film electrode can oxidize X-3B efficiently over a wide pH range, the photoelectrocatalytic experiment was investigated for five different initial pH values. Fig. 7 shows the effect of the pH of the dye solution on the PEC efficiency. In this section, the initial concentration of X-3B is 10 mg L^{-1}, the applied potential is 0.9 V and irradiation time is 25 min. All three samples show the same decrease of degradation efficiency of X-3B when the pH is increased from 3 to 9, and the degradation efficiency of three samples follow the same trend for all pH values: G-P25-2 > G-P25-3 > G-P25-1. The effects of pH on the photoelectrocatalytic degradation of X-3B are consistent with observations by other workers for the PEC degradation of humic acid [32] and for the PEC degradation pentachlorophenol [33] using different titania electrodes. pH influences the PEC process in many ways, such as varying the titania flat-band potential and changing the degree of adsorption of the target compound on the titania electrodes [33].

3.4. Stability of the graphene–titania film electrodes

To examine the stability of the as-prepared graphene–titania film electrodes, the PEC process was repeated 5 times with the same electrode (G-P25-2). In this section, the applied potential was fixed at 0.9 V (vs Ag/AgCl), the initial concentration of X-3B was 10 mg L^{-1} and the irradiation time was 25 min. Before each

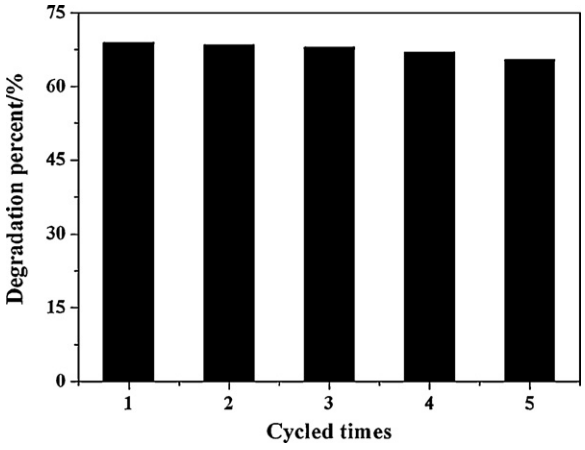

Fig. 8. The repeated utilization of G-P25-2 film electrode.

experiment, the used electrode was cleaned by dipping in ultrapure water for 2 h. The results, shown in Fig. 8, illustrate that the graphene–titania composite film electrode was very stable. There was just a slight decrease in the degradation percentage of X-3B after repeated utilizations. This can be explained as follows. Firstly, only a few graphene–titania nanoparticles peeled off in the photoelectrocatalytic degradation or cleaning process of the film electrode. Secondly, the film electrode was contaminated by dye molecules or intermediates or both. The consequent decrease in photoelectrocatalytic activity can be easily prevented by increasing the cleaning time or changing the cleaning solvent (such as ethanol). In addition, calcination of the film electrodes may enhance the fastness of the film, thus preventing peeling of the catalyst.

4. Conclusions

Graphene–titania composite film electrodes have been prepared and shown to exhibit better photoelectrocatalytic capacity for the degradation of dye X-3B in aqueous solution compared with a pure titania film electrode. The applied potential, pH and graphene content were shown to be important factors influencing the efficiency of the PEC process. X-3B degradation increased with increasing applied potential, but decreased with increasing pH.

Acknowledgments

We are grateful for grants from the National Key Basic Research Development Program ("973" project) of China (No. 2010CB429006), National Key Program of National Natural Science Foundation of China (No. 50830304), the National Key Basic Research Development Program ("973" project) of China (No. 2008CB418203), the National Natural Science Foundation of China (No. 51108158), Basic Research Project of Jiangsu Province (BK2008041).

References

[1] Y. Cong, X.K. Li, Y. Qin, Z.J. Dong, G.M. Yuan, Z.W. Cui, X.J. Lai, Carbon-doped TiO_2 coating on multiwalled carbon nanotubes with higher visible light photocatalytic activity, Appl. Catal. B: Environ. 107 (2011) 128–134.
[2] P. Li, Z. Wei, T. Wu, Q. Peng, Y.D. Li, Au-ZnO hybrid nanopyramids and their photocatalytic properties, J. Am. Chem. Soc. 133 (2011) 5660–5663.
[3] M. Brigante, P.C. Schulz, Remotion of the antibiotic tetracycline by titania and titania–silica composed materials, J. Hazard. Mater. 192 (2011) 1597–1608.
[4] J.J. Liu, W. Qin, S.L. Zuo, Y.C. Yu, Z.P. Hao, Solvothermal-induced phase transition and visible photocatalytic activity of nitrogen-doped titania, J. Hazard. Mater. 163 (2009) 273–278.
[5] J.G. Hou, Z. Wang, S.Q. Jiao, H.M. Zhu, 3D Bi12TiO20/TiO2 hierarchical heterostructure: synthesis and enhanced visible-light photocatalytic activities, J. Hazard. Mater. 192 (2011) 1772–1779.
[6] J.J. Xu, M.D. Chen, D.G. Fu, Study on highly visible light active Bi-doped TiO_2 composite hollow sphere, Appl. Surf. Sci. 257 (2011) 7381–7386.
[7] A. Fujishima, T.N. Rao, D.A. Tryk, Titanium dioxide photocatalysis, J. Photochem. Photobiol. C 1 (2000) 1–21.
[8] Q. Li, B.D. Guo, J.G. Yu, J.R. Ran, B.H. Zhang, H.J. Yan, J.R. Gong, Highly efficient visible-light-driven photocatalytic hydrogen production of CdS-cluster-decorated graphene nanosheets, J. Am. Chem. Soc. 133 (2011) 10878–10884.
[9] L.H. Ai, C.Y. Zhang, Z.L. Chen, Removal of methylene blue from aqueous solution by a solvothermal-synthesized graphene/magnetite composite, J. Hazard. Mater. 192 (2011) 1515–1524.
[10] H.D. Pham, V.H. Pham, T.V. Cuong, T.D. Nguyen-Phan, J.S. Chung, E.W. Shin, S. Kim, Synthesis of the chemically converted graphene xerogel with superior electrical conductivity, Chem. Commun. 47 (2011) 9672–9674.
[11] Y. Xu, H.Y. Gao, M.J. Li, Z.D. Guo, H.S. Chen, Z.H. Jin, B. Yu, Electronic transport in monolayer graphene with extreme physical deformation: ab initio density functional calculation, Nanotechnology 22 (2011) 365202.
[12] B.H. Chu, C.F. Lo, J. Nicolosi, C.Y. Chang, V. Chen, W. Strupinski, S.J. Pearton, F. Ren, Hydrogen detection using platinum coated graphene grown on SiC, Sensor. Actuat. B: Chem. 157 (2011) 500–503.
[13] S.R. Sun, L. Gao, Y.Q. Liu, Enhanced dye-sensitized solar cell using graphene–TiO(2) photoanode prepared by heterogeneous coagulation, Appl. Phys. Lett. 96 (2010) 083113.
[14] J.F. Shen, B. Yan, M. Shi, H.W. Ma, N. Li, M.X. Ye, One step hydrothermal synthesis of TiO(2)-reduced graphene oxide sheets, J. Mater. Chem. 21 (2011) 3415–3421.
[15] D.H. Yoo, T.V. Cuong, V.H. Pham, J.S. Chung, N.T. Khoa, E.J. Kim, S.H. Hahn, Enhanced photocatalytic activity of graphene oxide decorated on TiO_2 films under UV and visible irradiation, Curr. Appl. Phys. 11 (2011) 805–808.
[16] B. Neppolian, A. Bruno, C.L. Bianchi, M. Ashokkumar, Graphene oxide based Pt–TiO_2 photocatalyst: ultrasound assisted synthesis, characterization and catalytic efficiency, Ultrason. Sonochem. 19 (2011) 9–15.
[17] J. Du, X.Y. Lai, N.L. Yang, J. Zhai, D. Kisailus, F.B. Su, D. Wang, L. Jiang, Hierarchically ordered macro-mesoporous TiO(2)–graphene composite films: improved mass transfer, reduced charge recombination, and their enhanced photocatalytic activities, ACS Nano 5 (2011) 590–596.
[18] J.Q. Li, L. Zheng, L.P. Li, Y.Z. Xian, L.T. Jin, Fabrication of TiO_2/Ti electrode by laser-assisted anodic oxidation and its application on photoelectrocatalytic degradation of methylene blue, J. Hazard. Mater. 139 (2007) 72–78.
[19] Y.B. Liu, B.X. Zhou, J. Bai, J.H. Li, J.L. Zhang, Q. Zheng, et al., Efficient photochemical water splitting and organic pollutant degradation by highly ordered TiO_2 nanopore arrays, Appl. Catal. B: Environ. 89 (2009) 142–148.
[20] F.M.M. Paschoal, M.A. Anderson, M.V.B. Zanoni, Simultaneous removal of chromium and leather dye from simulated tannery effluent by photoelectrochemistry, J. Hazard. Mater. 166 (2009) 531–537.
[21] J.P. Li, X. Zhang, Z.H. Ai, F.L. Jia, L.Z. Zhang, J. Lin, Efficient visible light degradation of Rhodamine B by a photo-electrochemical process based on a Bi_2WO_6 nanoplate film electrode, J. Phys. Chem. C 111 (2007) 6832–6836.
[22] Z.H. Xu, J.G. Yu, Visible-light-induced photoelectrochemical behaviors of Fe-modified TiO_2 nanotube arrays, Nanoscale 3 (2011) 3138–3144.
[23] H.M. Zhang, X.L. Liu, Y.B. Li, Q.F. Sun, Y. Wang, B.J. Wood, et al., Vertically aligned nanorod-like rutile TiO_2 single crystal nanowire bundles with superior electron transport and photoelectrocatalytic properties, J. Mater. Chem. 22 (2012) 2465–2472.
[24] K.Y. Cheung, C.T. Yip, A.B. Djurisic, Y.H. Leung, W.K. Chan, Long K-doped titania and titanate nanowires on Ti foil and fluorine-doped tin oxide/quartz substrates for solar-cell applications, Adv. Funct. Mater. 17 (2007) 555–562.
[25] H. Nishikiori, Y. Uesugi, N. Tanaka, T. Fujii, Photo-electric conversion in dye-doped nanocrystalline titania films, J. Photochem. Photobiol. A: Chem. 207 (2009) 204–208.
[26] T.H. Zhang, S.L. Zhao, L.Y. Piao, Z. Xu, X.D. Liu, C. Kong, et al., Preparation of porous titania film and its application in solar cells, J. Nanosci. Nanotechnol. 11 (2011) 9745–9748.
[27] J.L. Wu, X.P. Shen, L. Jiang, K. Wang, K.M. Chen, Solvothermal synthesis and characterization of sandwich-like graphene/ZnO nanocomposites, Appl. Surf. Sci. 256 (2010) 2826–2830.
[28] G. Williams, B. Seger, P.V. Kamat, TiO_2–graphene nanocomposites. UV-assisted photocatalytic reduction of graphene oxide, ACS Nano 2 (2008) 1487–1491.
[29] X.Y. Zhang, H.P. Li, X.L. Cui, Y.H. Lin, Graphene/TiO_2 nanocomposites: synthesis, characterization and application in hydrogen evolution from water photocatalytic splitting, J. Mater. Chem. 20 (2010) 2801–2806.
[30] H. Zhang, X.J. Lv, Y.M. Li, Y. Wang, J.H. Li, P25–graphene composite as a high performance photocatalyst, ACS Nano 4 (2010) 380–386.
[31] L.C. Chen, Y.C. Ho, W.S. Guo, C.M. Huang, T.C. Pan, Enhanced visible light-induced photoelectrocatalytic degradation of phenol by carbon nanotube-doped TiO_2 electrodes, Electrochim. Acta 54 (2009) 3884–3891.
[32] X.Z. Li, F.B. Li, C.M. Fan, Y.P. Sun, Photoelectrocatalytic degradation of humic acid in aqueous solution using a Ti/TiO_2 mesh photoelectrode, Water Res. 36 (2002) 2215–2224.
[33] X. Quan, X.L. Ruan, H.M. Zhao, S. Chen, Y.Z. Zhao, Photoelectrocatalytic degradation of pentachlorophenol in aqueous solution using a TiO_2 nanotube film electrode, Environ. Pollut. 147 (2007) 409–414.